Strong Shear Flow-Driven Simultaneous Formation of Classic Shish-Kebab, Hybrid Shish-Kebab, and Transcrystallinity in Poly(lactic acid)/Natural Fiber Biocomposites

ARTICLE *in* ACS SUSTAINABLE CHEMISTRY & ENGINEERING · OCTOBER 2013

Impact Factor: 4.64 · DOI: 10.1021/sc4003032

8 AUTHORS, INCLUDING:

Huan Xu
Sichuan University
21 PUBLICATIONS **121** CITATIONS
SEE PROFILE

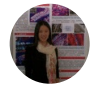

Lan Xie
The University of Sheffield
12 PUBLICATIONS **66** CITATIONS
SEE PROFILE

Ganji Zhong
Sichuan University
163 PUBLICATIONS **4,505** CITATIONS
SEE PROFILE

Benjamin S Hsiao
Stony Brook University
572 PUBLICATIONS **20,614** CITATIONS
SEE PROFILE

ACS Sustainable Chemistry & Engineering

Research Article

pubs.acs.org/journal/ascecg

Strong Shear Flow-Driven Simultaneous Formation of Classic Shish-Kebab, Hybrid Shish-Kebab, and Transcrystallinity in Poly(lactic acid)/Natural Fiber Biocomposites

Huan Xu,[†] Lan Xie,[†] Yan-Hui Chen,[†] Hua-Dong Huang,[†] Jia-Zhuang Xu,[†] Gan-Ji Zhong,*[,†] Benjamin S. Hsiao,[‡] and Zhong-Ming Li*[,†]

[†]College of Polymer Science and Engineering, State Key Laboratory of Polymer Materials Engineering, Sichuan University, Chengdu 610065, Sichuan, People's Republic of China

[‡]Department of Chemistry, Stony Brook University, Stony Brook, New York 11794-3400, United States

Supporting Information

ABSTRACT: A strong continuous shear flow was imposed on the melt of ramie fiber reinforced poly(lactic acid) (PLA) biocomposites during practical processing. Classic shish-kebabs and typical transcrystallinity were simultaneously formed in the sheared PLA/ramie fiber samples, which were closely related to formation of row-nuclei induced by the strong shear flow that was further amplified by incorporated natural fibers. Interestingly, some nano-sized ultrafine ramie fibers tended to absorb and stabilize the as-formed row-nuclei, which subsequently grew into the unexpected hybrid shish-kebabs. We proposed that the formation of hybrid shish-kebabs underwent the process of "capturing extended chain bundles for hybrid shishes" with the applied shear flow acting as the driving force. Further attempts were made to understand their contribution to the mechanical performances. With the existence of transcrystallinity, PLA/fiber interfacial adhesion was considerably enhanced. Meanwhile, positive reinforcing and toughening effects could originate from the shish-kebabs and hybrid shish-kebabs with extended chain bundles. Consequently, a noteworthy enhancement in tensile strength, tensile modulus, storage modulus, and impact toughness was achieved in the modified biocomposites, obtaining a substantial increase of 14.0%, 8.4%, 23.4%, and 90.4%, respectfully, compared to the control biocomposite. These results clearly demonstrated that the precisely controlled interfacial crystalline structures under industrial conditions of processing are highly beneficial to the mechanical performances.

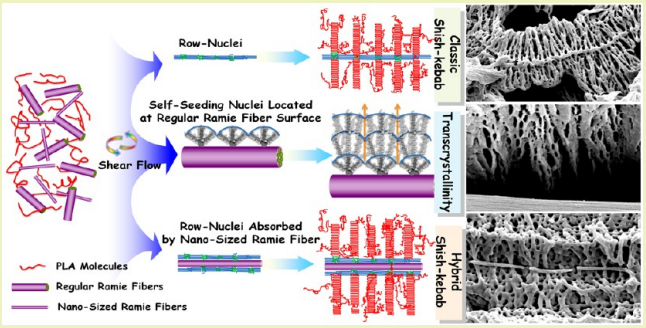

KEYWORDS: *Poly(lactic acid), Natural fiber, Interfacial superstructure, Shear flow*

INTRODUCTION

Poly(lactic acid) (PLA) has been consolidating its status as the front runner in the emerging bioplastics market with easy availability and an attractive cost-performance ratio.[1−3] Developing desirable biocomposites based on PLA and renewable natural fibers is a promising strategy toward reducing costs and improving bulk performance, while the satisfying biodegradability is absolutely preserved.[4−6] The distinct advantages of utilizing natural fibers to reinforce PLA not only lie in their excellent mechanical properties but also are embodied in the strong capacity of natural fibers in tailoring the crystalline morphology of PLA.[7]

It is widely known that the crystalline morphology formed at the interfaces between the polymer matrix and foreign fibers has a significant influence on the mechanical properties of composite materials.[8,9] The surface of the fibers has a high heterogeneous nucleation activity, and thus, a vast number of nuclei formed on the surface will hinder the lateral extension of lamellae and force them to grow in one direction, resulting in the formation of a columnar crystalline layer perpendicular to the axis of fiber surface.[8,10] This is known as transcrystallinity, which is featured as a stronger and stiffer layer with preferred orientation relative to the axis of the fiber.[11,12] Thereby, the loads can be transferred from the matrix across the interphase in an efficiently favorable manner due to the enhanced fiber/matrix adhesion. Extending this point of view, the latest research interests are attracted to foster PLA transcrystallinity under favorable isothermal cystallization conditions induced by natural fibers such as sisal fiber,[13] flax fiber,[14] and ramie fiber,[15] which can provide abundant heterogeneous nucleation sites. Nevertheless, when it comes to the case of fabricating PLA-based biocomposites by common processing (e.g., extrusion compounding followed by injection molding,) which must experience extremely rapid cooling rates, it is still a great

Received: August 17, 2013
Revised: September 16, 2013
Published: September 21, 2013

challenge to produce high crystallinity (usually less than 20%) and transcrystallinity because of the undesirable crystallization conditions.[15]

It seems we are in a dilemma that an industrially feasible manufacturing process for mass production of PLA biocomposites and a desirable crystalline morphology for superior performance cannot be achieved at once. Naturally, it stimulates us to pursue some breakthroughs to industrially develop high-performance biocomposites associated with enhanced interfacial properties. Our recent explorations on optimizing the crystalline morphology of PLA by applying an intense shear flow field probably shed light on the approach to tackle this present issue.[16,17] As general knowledge, the imposed shear flow could trigger dramatic enhancement of crystallization kinetics for semi-crystalline polymers.[18] Polymer chains tend to extend along the flow direction, leading to the formation of a great quantity of highly oriented row-nuclei ahead of the formation of shish-kebab structures.[18] It is also suggested that once spherulitic texture is transformed to a shish-kebab superstructure, significant improvement in tensile strength, stiffness, ductility, toughness, heat defection temperatures, and barrier properties can be achieved in various semi-crystalline polymers.[19,20] However, for PLA presenting relatively short chain lengths and semi-rigid molecular backbones, a weak shear flow provided by experimental shear hot-stage cannot sufficiently trigger the transformation of crystalline morphology into oriented shish-kebab superstructures.[21] Recently, by exploiting the strong shear flow field existing in the modified injection molding, namely, oscillation shear injection molding (OSIM), we found a powerful force to effectively stretch and orient PLA chains. As a result, the formation of rich PLA shish-kebabs and thereby remarkable improvement of overall performance was put into evidence.[16]

Having realized the huge potential of intense shear flow, we reasonably suppose such that an applied shear flow is prone to significantly alter the morphologies of PLA/natural fiber biocomposites; natural fibers in the flowing PLA melts tend to easily align along the flow direction owing to the intrinsically considerable flexibility of ramie fibers,[15] while PLA chains in the molten state are forced to extend and orient parallel to those well-aligned fibers. By providing abundant nucleation sites on the surfaces of natural fibers,[13] stretched PLA chains would locate at these sites to fold and pack to form a sequence of crystalline domains, constituting the interfacial structure of row-nuclei onto which lamellae probably afterward develop to columnar transcrystallinity superstructures due to spatial restriction of compact nuclei.[22] Thus, the aligned fibers and extended PLA chains actually perform a synergistic effect to generate oriented transcrystallinity superstructures involving folded-chain crystallization.

In order to examine the hypothesis of the formation of PLA transcrystallinity under the coexistence of natural fibers and shear flow, we attempt to utilize the intense shear flow existing in OSIM technology to manipulate the morphology of PLA/ramie fiber biocomposites in this work. On the basis of direct morphological observations, which are described below, we demonstrate for the first time, in an industrial type of processing, that such a continuous shear flow not only improves the orientation degree of ramie fibers but also stretches and orients PLA molecules, leading to the direct achievement of both transcrystallinity superstructure and classic shish-kebab superstructure in PLA biocomposites. Intriguingly enough, in this work, a rigorous observation unearths the unprecedented hybrid shish-kebab superstructure of PLA induced by the ultrafine fibers sparsely existing in the ramie fibers, displaying a cylindrical symmetry with transverse lamellae growing from the central linear nanofibers. Hybrid shish-kebabs of other polymer system display a highly similar appearance with that of the classic shish-kebab, as well as remarkable contributions to material performances.[23−26]

EXPERIMENTAL SECTION

Materials. PLA under a trade name of 4032D comprising around 2% D-LA was commercially purchased from Nature Works, which has a weight-average molecular weight and number-average molecular weight of 2.23×10^5 g/mol and 1.06×10^5 g/mol, respectively. Ramie fibers used were bast fibers from the outer culm of the ramie plant with a density of 1.5 g/cm^3, moisture content of 9%, tensile strength of ∼450 MPa, and modulus of ∼23 GPa, which were kindly supplied by Yuzhu Plant Fiber Industrial Co. Ltd., Sichuan Province, China, and were used as received without further treatment. The digital images of ramie fibers showing the topographic characters are depicted in Figure S1 of the Supporting Information.

Sample Preparation. PLA biocomposites containing 10 wt % ramie fibers were fabricated by extrusion compounding followed by injection molding, while pure PLA subjected to the same processing conditions was also prepared to make blank control samples. In order to avoid the degradation due to hydrolysis and prevent the formation of voids during processing, ramie fibers, PLA, and their blends were dried at 100 °C under vacuum overnight before extrusion or injection molding. The compounding process was carried out in a co-rotating twin screw extruder (Nanjing Rubber & Plastics Machinery Plant Co. Ltd., China) with a ratio of screw length to its diameter (L/D) of 40. Temperatures in seven zones were set at 120, 160, 170, 170, 170, 165, and 165 °C from feed section to metering section, respectively, and the screw speed was constantly held at 150 rpm in order to achieve stable melt flow and avoid thermal degradation of PLA. The threadlike ramie fibers were fed into another port located in a barrel of section 3 after the melting of PLA, and the fiber contents in biocomposites were fixed at 10 wt %, which were adjusted by the feeding speed of PLA and ramie fibers.

The extruded pellets after drying were injection molded into standard double-bone test samples; the barrel temperature profiles were set at 130, 160, 180, 185, and 180 °C from hopper to nozzle, respectively. The key feature in our strategy involves the utility of a modified injection molding, namely, oscillation shear injection molding (OSIM) technology.[19] During the packing stage of the injection molding process, a controlled shear flow was continuously imposed on the melt by using OSIM technology, which had two hydraulically actuated pistons that move reciprocally at the same frequency of 0.3 Hz and the pressure of 15 MPa, and the shear flow did not cease until the gate of the mold solidified. Detailed information of the OSIM machine is available in our previous work.[19] Without applying the oscillation shear, corresponding counterparts were prepared by conventional injection molding (CIM). It should be noticeable that the control samples of neat PLA and reinforced PLA biocomposites subjected to the same thermal conditions were also prepared (i.e., the case without oscillation shear flow). The cycle time of the sample preparation by OSIM and CIM was fixed at about 3 min in this study. The mold temperature was held at 50 °C with the aid of an automatic temperature control system during the whole cycles for both OSIM and CIM processing. For the sake of briefness, the resultant injection-molded pure PLA and biocomposite samples prepared by the two processing methods will be referred as C-PLA, O-PLA, C-PLA10, and O-PLA10. For instance, O-PLA10 stands for the sample of PLA/ramie fiber biocomposite prepared by OSIM, while C-PLA represents the sample of pure PLA molded by CIM. The thickness of the injection-molded samples is 4 mm.

Moreover, single ramie fiber-reinforced PLA samples were prepared in order to evaluate the transcrystallinity texture formed during quiescent and shear-induced crystallization. Specifically, dried PLA was dissolved in dichloromethane (CH_2Cl_2). Then the solution was

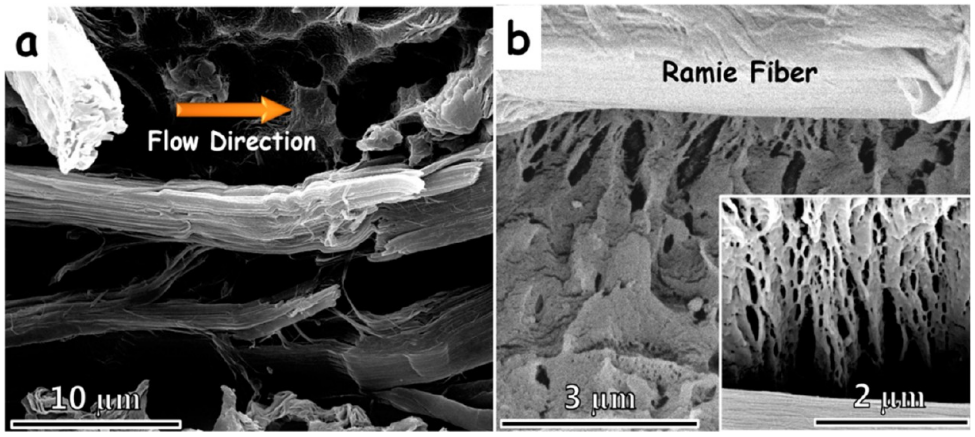

Figure 1. SEM observations of crystalline morphology in the vicinity of ramie fibers of injection-molded PLA/ramie fiber biocomposites: (a) C-PLA10 and (b) O-PLA10. Inset depicts the high-resolution micrograph of the oriented lamellae originated from the ramie fiber. The flow direction is horizontal.

carefully dripped onto a sheet glass, and the solvent was volatilized absolutely at 30 °C under vacuum for 6 h. Finally a thin film with a thickness of approximately 10 μm was generated. A single ramie fiber with a diameter of about 17 μm was sandwiched between two pieces of the aforementioned PLA film and heated by a Linkam CSS450 hot stage (Linkam Scientific Instruments, U.K.) at 200 °C for 5 min and then cooled rapidly to 136 °C. The shear flow-induced crystallization sample was fostered at 136 °C for 40 min after gently pulling the ramie fiber at a constant rate of about 0.2 cm/s for 5 s. Additionally, a quiescent crystallization sample that endured an isothermal crystallization at 136 °C for 40 min was also prepared as the control sample.

Characterization and Testing. *Scanning Electronic Microscopy (SEM).* To get a clear observation of the crystalline morphology in the injection-molded samples, a small block was cut from the injection-molded part first, and then the block was cryogenically fractured along the midcourt line in the flow direction after staying in liquid nitrogen for 0.5 h. The smooth fracture surface was etched by a water−methanol (1:2 by volume) solution containing 0.025 mol/L of sodium hydroxide for 12 h at 25 °C; subsequently, the etched surface was cleaned by using distilled water and ultrasonication. Herein, we are mainly concerned with the crystalline morphology formed in the oriented layer that is 400−800 μm far from the surface of the injection-molded parts of PLA biocomposites. Similarly, the quiescent and shear flow-induced crystallization samples were etched in the mixture solution under the same conditions. A field-emission SEM (Inspect F, FEI, Finland) was utilized for all samples, which were sputter-coated with gold before observations, and the accelerated voltage was held at 5 kV.

Two-Dimensional Small-Angle X-ray Scattering (2D-SAXS). 2D-SAXS measurements were conducted at the beamline BL16B1 of Shanghai Synchrotron Radiation Facility (SSRF, Shanghai, China) to examine the superstructure of PLA in the oriented layer of injection-molded biocomposites, and the explicit sample preparation is presented in our previous work.[16] The 2D-SAXS images were collected with an X-ray CCD detector (Model Mar165, 2048 pixels × 2048 pixels of 80 μm × 80 μm). The sample-to-detector distance was held at 1900 mm, while the monochromated X-ray beam operated at a constant wavelength of 0.124 nm. The radically integrated intensities $I(q)$ ($q = 4\pi\sin\theta/\lambda$) are obtained for integration in the azimuthal angular range of a whole circle, where 2θ represents the scattering angle and λ represents the wavelength of X-ray.

Differential Scanning Calorimeter (DSC). A DSC Q200 (TA Instruments, U.S.A.) was used to probe the thermal properties such as melting and crystallization behaviors for PLA and the PLA/ramie fiber biocomposites. Samples of the neat PLA and the biocomposites (around 5−6 mg), obtained from the oriented layer of the injection-molded bars, were heated from 30 to 180 °C at a heating rate of 5 °C/min under nitrogen atmosphere. The crystallinity (χ_c) can be calculated by subtracting the enthalpy of cold crystallization and premelt crystallization from the enthalpy of melting by using eq 1.[27]

$$\chi_c = \frac{\Delta H_m - \Delta H_{cc} - \Delta H_{pc}}{\Delta H_m^0} \times 100\% \quad (1)$$

where ΔH_m is the enthalpy of melting for PLA, ΔH_{cc} is the enthalpy of cold crystallization, ΔH_{pc} is the enthalpy of premelt crystallization, and ΔH_m^0 is the enthalpy of melting for a 100% crystalline PLA taken as 93.7 J/g.[28]

Polarized Optical Microscopy (POM). POM was carried out to observe the crystalline morphology in the vicinity of ramie fiber after quiescent and shear flow-induced crystallization. An Olympus BX51 polarizing optical microscopy (Olympus Co., Tokyo, Japan) equipped with a MicroPublisher 3.3 RTV CCD was applied to observe the crystalline morphology of the quiescent and shear flow-induced crystallization samples.

Mechanical Property Testing. The tensile testing was carried out at room temperature using an Instron universal test instrument (Model 5576, Instron Instruments, U.S.A.) with a crosshead speed of 5 mm/min and a gauge length of 20 mm (the ASTM standard D638). The notched Izod impact tests were carried out according to the GB/T 1843-08 standard at room temperature, and the dimensions of testing specimens were carefully machined to be 50 mm × 6 mm × 4 mm with a V-notch. A minimum of six replicates for each sample were tested at the same conditions, and the average values were presented with standard deviation.

RESULTS AND DISCUSSION

Crystalline Morphologies of PLA/Ramie Fiber Biocomposites Under Intense Flow. To obtain a clear understanding of the crystalline morphology of injection-molded biocomposites developed in the intensive shear flow, Figure 1 gives the direct observations by employing a high-resolution SEM. Figure 1a clearly manifests no trace of transcrystallinity around ramie fibers nor the presence of crystals in the bulk in the case of C-PLA10 samples. The poor crystalline behavior and imperfect crystalline morphology evidently reveal the huge difficulty for PLA to develop preferential crystalline morphology during the common processing, which essentially arises from the undesirable crystallization ability of PLA.[15] In direct contrast to the common injection-molded biocomposite sample, Figure 1b shows the ramie fiber is closely wrapped by a layer of oriented lamellae perpendicular to the fiber, displaying the classic features of transcrystallinity superstructure. Evidently, compact

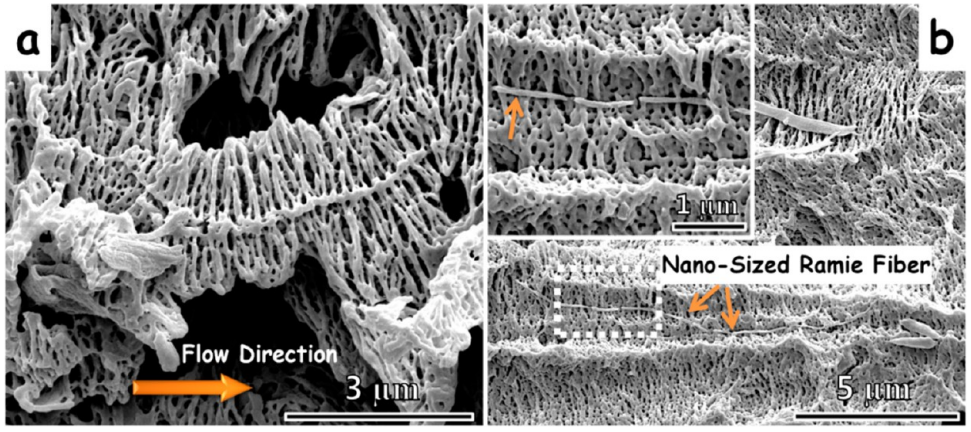

Figure 2. SEM observations of (a) self-nucleated shish-kebab and (b) nano-sized ramie fiber-induced hybrid shish-kebab superstructure formed in the O-PLA10 sample. Inset of (b) presents the high-resolution micrograph of local morphology in the white dashed rectangle. The flow direction is horizontal.

transcrystallinity is actually achieved in the OSIM biocomposite sample, which generates on the surface of the ramie fiber with a radius of 2−5 μm. Generally, the formation of transcrystallinity starts at the interface due to the strong heterogeneous nucleation ability of fibers, and the subsequent growth of lamellae is restricted in the lateral direction.[29] However, in our case, transcrystallinity formed in O-PLA10 must not be attributed to the nature of the nucleation ability of ramie fibers due to the absence of transcrystallinity in C-PLA10. The crucial difference comes from the intensity of flow field produced by CIM and OSIM processing. Therefore, we tentatively believe that the strong shear flow provided by OSIM can prominently boost the formation and growth of transcrystallinity on the surface of oriented fibers in an energetically favorable manner.

It is worthwhile stating that it is the first time to directly observe transcrystallinity superstructures in injection-molded PLA/natural fiber biocomposites, from which we can reasonably expect an improved interfacial adhesion and thus enhanced mechanical properties.[8,9] A large amount of experimental research is spent to modify natural fibers through physical and chemical treatments such as microwaving, mercerization, surface-grafting, coupling, and alkalization.[7,30] However, being extremely time consuming, these reported modifications cannot fit well the industrial processing. What is worse, the consumption of tons of noxious and toxic reagents goes against the original intention to develop environmentally benign biocomposites based on green resources. The methodology proposed herein, in effect, holds great potential in conveniently manufacturing biocomposites with favorable interfacial strength on a large scale.

Further insights into the crystalline morphology of the OSIM biocomposite sample were directly acquired by SEM observations. In the matrix, a typical shish-kebab superstructure is obtained as clearly illustrated in Figure 2a. Displaying a cylindrical symmetry with regularly aligned lamellae growing from the central shish, the shish-kebab presents a diameter of approximately 2 μm. It evidently reveals that shish-kebabs can be created in injection-molded parts of natural fiber reinforced PLA biocomposites by introducing an intense shear flow. Under the enhanced shear flow provided by the OSIM processing, we recently gained rich cylindrical shish-kebabs in the subskin, oriented and intermediate layers (50−1200 μm far from the surface) for pure PLA and plasticized PLA, respectively.[16] By comparing the morphology of shish-kebab structures formed in various systems, it is worth stressing that the diameter of the shish-kebab formed in the OSIM biocomposite sample (∼2 μm) is nearly three times as large as that of the OSIM PLA sample (∼0.7 μm). The increment of shish-kebab size is probably attributed to the decreased quantity of shishes formed in the system of the biocomposite. Acting as a favorable self-reinforced element, the shish-kebab superstructure is widely demonstrated to make a notable contribution to the mechanical properties of the semicrystalline polymer.[16,20] Pioneering work launched by Kalay and Bevis,[31,32] later studied by Fu Q. et al.,[33] and recent progress gained in our laboratory[19] found sufficient evidence for its self-reinforcing effects. We herein verified the possibility of developing shish-kebabs in an injection-molded biocomposite system under an intensive shear flow field, and the reinforcing effects of shish-kebabs in the biocomposites are worthwhile anticipating, which will be illustrated in the following context.

Besides the observation of transcrystallinity and shish-kebab superstructures, unexpectedly, Figure 2b reveals the existence of a hybrid shish-kebab superstructure. The nano-sized fiber as a shish is wrapped by regularly aligned kebabs perpendicular to the axis. Strictly oriented PLA crystal lamellae (so-called kebabs) are periodically decorated on an ultrafine ramie fiber, which presents the diameter in nanoscale. The kebabs show the approximately same diameter (1.9 μm) with those of classic shish-kebabs (2 μm), evidently indicating the kebabs in the classic and hybrid shish-kebab superstructures must have nucleated at about the same time and experienced the same period of growth. As for the ultrafine ramie fiber, it should be noted that ramie fibers must experience fierce friction, shear, and elongation flow along with intense heating during the fabrication of the biocomposites (i.e., extrusion compounding followed by injection molding), allowing them to be torn into ultrafine fibers with a drastically decreased diameter.[15] The formaion of ultrafine nanofibers was also confirmed by SEM (Figure S2, Supporting Information)

To the best of our knowledge, an up-to-date clear picture of a natural fiber-induced PLA hybrid shish-kebab superstructure has not been reported. A hybrid shish-kebab of another polymer system has a highly similar appearance with that of the classic shish-kebab.[23−26] Various approaches, mostly in the last years, have been reported to attain hybrid shish-kebabs, such as isothermal and nonisothermal crystallization in dilute polymer

solutions,[23,34] epitaxy growth of lamellae induced by supercritical carbon dioxide,[35] and nanotube-induced hybrid shish-kebabs in polymer melts under a flow field.[36] As reported, carbon nanotubes are preferentially selected to serve as the central shish to induce the folding and packing of polymer chains into columnar lamellae perpendicular to the nanotubes. In this work, natural nanofibers have been demonstrated to be able to act as the hybrid shish in a way like carbon nanotubes, which could be useful for the increasingly appreciated field of cellulose nanofibers and nanowhiskers in terms of their wide availability from a variety of renewable bioresources, desirable biodegradability, unique surface properties, excellent mechanical performance, and low density.[37,38]

The above morphological observations suggest the simultaneous formation of transcrystallinity and self-nucleated shish-kebab and hybrid shish-kebab superstructures under the synergistic effects of ramie fibers and external intense shearing. To obtain quantitative insights into the crystalline morphology in injection-molded PLA/ramie fiber biocomposite parts, 2D-SAXS measurements were further performed. Figure 3 depicts

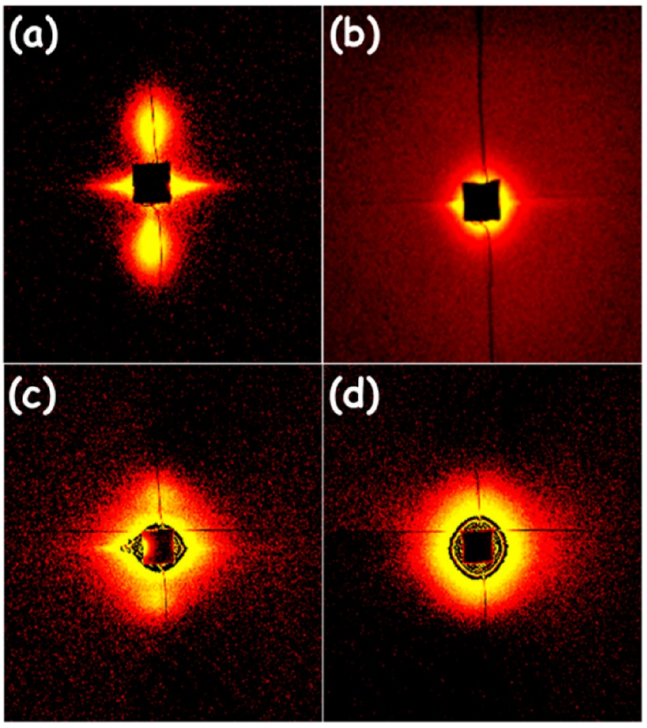

Figure 3. Representative 2D-SAXS patterns of injection-molded pure PLA and PLA/ramie fiber biocomposites: (a) O-PLA, (b) C-PLA, (c) O-PLA10, and (d) C-PLA10.

the representative 2D-SAXS patterns. For the O-PLA sample (Figure 3a), equatorial streaks and meridional lobes are clearly observed, which confirm again the formation of PLA shish-kebab structures parallel to the flow direction and the growth of kebabs perpendicular to the shish axis through the folded-chain crystallization process, respectively. The equatorial diffraction intensity of O-PLA10 moderately weakens in the 2D-SAXS pattern as illustrated in Figure 3c, which is consistent with the increased diameter observed by SEM. Both results confirmed the decreased quantity of self-nucleated shishes in the system of biocomposites. Meanwhile, Figure 3c reveals that there exists two obvious bulb-shape lobes in the meridional direction of the 2D-SAXS image of O-PLA10, attributing to the product of oriented kebabs perpendicular to the flow direction in self-nucleated shish-kebabs and nano-sized ramie fiber-induced hybrid shish-kebabs. Nevertheless, Figure 3b and d demonstrate that no scattering reflection can be found in either C-PLA or C-PLA10 samples, probably resulting from the random orientation of the lamellae with a large distribution of lamellar distance. Under the weak shear flow field during CIM processing, the lamellar structure fails to develop the preferential orientation and randomly distributes in the bulk. Thus, 2D-SAXS patterns and SEM observations yield the well-consistent results in probing into the crystalline morphology.

In order to further examine the lamellar structures in PLA/ramie biocomposites containing shish-kebabs and transcrystallinity, the long period regarding the lamellar structure is calculated using the Bragg equation, $L = 2\pi/q^*$, where L indicates the long period, and q^* stands for the peak position in the scattering curves. Figure 4 describes the SAXS intensity

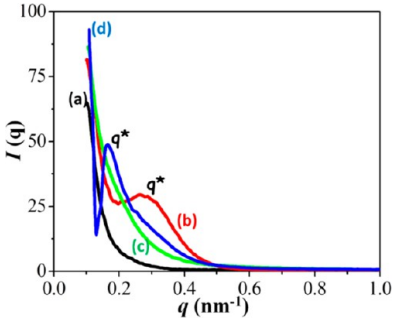

Figure 4. 1D-SAXS curves showing the corresponding intensity profiles of the scattering patterns of Figure 3: (a) C-PLA, (b) O-PLA, (c) C-PLA10, and (d) O-PLA10.

curves. It clearly suggests that only the OSIM samples containing oriented lamellae present distinct peaks. Specifically, the O-PLA sample shows a maxima at around $q = 0.3$ nm^{-1}, while the maxima sharply shifts to $q = 0.18$ nm^{-1} for the O-PLA10 sample, i.e., the long periods for the O-PLA and O-PLA10 samples are 22.8 and 38.1 nm, respectively. The drastic increase of 15.2 nm suggests that the presence of ramie fibers can increase lamellar spacing between adjacent regular lamellae. Besides the direct SEM morphological observation, the quantitative analyses of SAXS results further verify the creation of transcrystallinity structure in the vicinity of ramie fibers from the viewpoint of lamellar characters. With regards to the nucleation ability, regular ramie fibers cannot match the nano-sized ramie fibers and extended nanostructured shish in providing available nucleating sites and sufficient surface interactions and energy to absorb the folded-chain lamellae. As a consequence, the transcrystallinity texture developed at the fiber surface, compared to the self-nucleated shish-kebabs and hybrid shish-kebabs, presents less compact lamellae. It must be responsible for the significant increase in the long spacing of O-PLA10 containing transcrystallinity and shish-kebabs. A similar phenomenon was also observed in shear-induced crystallization of isotactic polypropylene composites containing aramid fibers by Larin and co-workers.[22]

Figure 5 illustrates the DSC heating scans for the four samples at a heating rate of 5 °C/min. Apparently, four main transitions are successively displayed on the curves of C-PLA and C-PLA10: a glass transition at a temperature adjacent to 57 °C (T_g), a cold crystallization peak near 91 °C (T_{cc}),

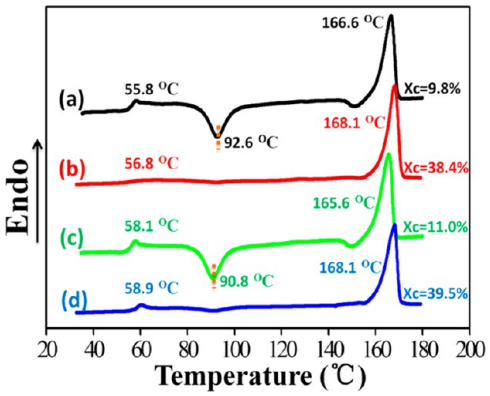

Figure 5. DSC heating traces of injection-molded pure PLA and PLA/ramie fiber biocomposites: (a) C-PLA, (b) O-PLA, (c) C-PLA10, and (d) O-PLA10. Thermal parameters, including the glass transition temperature (T_g), cold crystallization temperature (T_{cc}), melting point (T_m), and crystallinity (X_c) formed in injection molding, are marked around the DSC curves. Note that all values of the crystallinity are normalized values based on the matrix content.

subsequently a small secondary crystallization exotherm with a maximum rate around 150 °C (T_{sc}), and finally, a melting endotherm with a maximum rate at about 166 °C (T_m).[27] Interestingly, no obvious traces of cold crystallization and secondary crystallization before melting are observed for O-PLA and O-PLA10 samples. Combining the SEM and DSC results, it is easy to conclude that shear flow-induced crystallization can significantly increase the crystallinity from 9.8% for C-PLA to 38.4% for O-PLA. Note that such a remarkable increase in crystallinity of the PLA part during injection molding is rarely observed. The enhanced crystallization under the synergistic effects of shear flow, regular ramie fibers, and nano-sized ramie fibers can further promote the crystallinity, slightly increasing from 11.0% for C-PLA10 to 39.5% for O-PLA10 containing transcrystallinity, shish-kebabs, and hybrid shish-kebabs. Meanwhile, some additional noteworthy phenomena are also revealed by DSC. We clearly observe an obvious rise of T_m in OSIM samples (both are 168.1 °C), compared to 166.6 and 165.6 °C for C-PLA and C-PLA10, respectively, due to the high thermal stability of highly oriented shish-kebabs.[36] Distinctly, the addition of ramie fibers appears to hinder the chain mobility. The T_g of C-PLA10 and O-PLA10 biocomposites containing ramie fibers, which experience glass transitions at 56.8 and 58.9 °C, is 1.0 and 0.8 °C higher than that of C-PLA and O-PLA, respectively. It is plausible that the driving force for the restrained PLA chains is the geometric confinement effect of ramie fibers. These fibers can drastically disturb the continuity of the bulk matrix and hinder chain motions. Additionally, the considerable interfacial interactions between polymer chains and ramie fibers could also constrain the mobility of PLA chains.[15,39] On the other hand, a noticeable decrease in T_{cc} (~1.8 °C) for C-PLA10 compared to C-PLA is clearly observed, demonstrating that ramie fibers strongly play a positive role in the crystallization kinetics of PLA.

Mechanism for the Formation of Multiform Crystalline Superstructures in PLA Biocomposites Driven by Shear Flow. It is constructive to discuss the crystalline morphologies of the matrix formed under the combined effects of the shear flow field and ramie fibers, which, unfortunately, are still poorly understood so far.

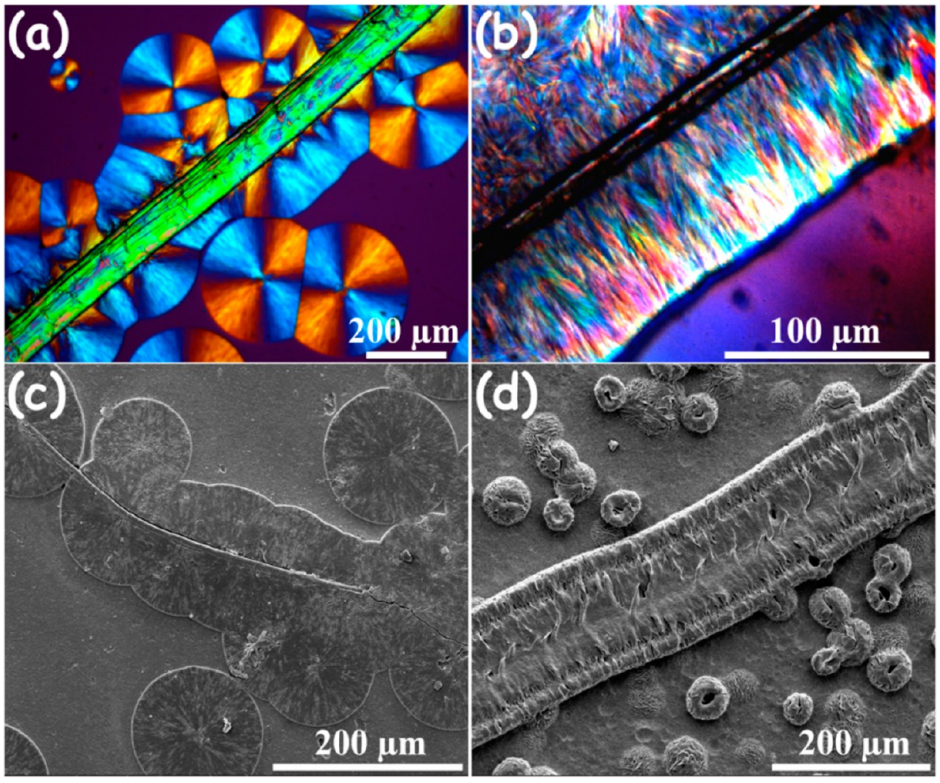

Figure 6. POM and SEM observations of a transcrystallinity superstructure formed at the ramie fiber surface during the quiescent (a, c) and shear flow-induced (b, d) crystallization. The quiescent crystallization samples were held at 136 °C for 40 min, while the shear flow-induced crystallization samples were fostered at 136 °C for 40 min after gently pulling the ramie fiber at a constant rate of about 0.2 cm/s for 5 s.

For the formation of the classic shish-kebab superstructure of PLA, it undoubtedly shares the same mechanism with that of polyethylene and polypropylene in the flow field, deducing from the high similarity in cylindrical morphology and scattering patterns. Compared to polyolefins, PLA has relatively short and semi-rigid chains with low steric regularity; thus, it is difficult to develop shish-kebab superstructures. Taking advantage of the in-mold shearing action provided by the OSIM technique accompanied by the fast cooling to freeze and stabilizing the established shish precursors, the PLA chains (or molecular chain networks) under the intense shear flow field tend to deform along the flow direction and thus are highly oriented and well packed to form a sequence of quasi-crystalline nanodomains, assembling into the inner structure of row-nuclei and shish, onto which lamellae may afterward develop disc-shaped kebabs perpendicular to the shish.[40,41] It is clear that ramie fibers cannot disturb the regular development of oriented shish-kebabs, following the widely discussed shear-induced crystallization procedure.

For the formation of transcrystallinity induced by ramie fibers with a diameter ranging from several to tens of micrometers, the concerted effects of ramie fiber and shear flow are believed to be a driving force. Naturally, there exists a high density of heterogeneous nucleation sites at the surface of the ramie fiber, which provides a vital prerequisite for adjacent chains to settle down and nucleate.[15] However, during the injection molding that endures rapid cooling and short cycle time (~3 min), only the presence of ramie fiber is unable to develop transcrystallinity for PLA with a semi-rigid molecular backbone and poor chain mobility. Therefore, we cannot find any traces of transcrystallinity in the C-PLA10 sample (Figure 1a). As long as the PLA biocomposites are continuously subjected to the intense shear flow during OSIM processing, ramie fibers tend to align more regularly along the flow direction, especially for the inner zone close to the core layer as evidently depicted in Figure S3 of the Supporting Information. Moreover, the energy barrier for nucleation drastically drops after the PLA chains deform and orient along the flow direction. The flow-induced self-seeding nucleation in advance will facilitate the crystallization kinetics of PLA by a high concentration of stretched chains, which can be further enhanced by a possible local shearing field near the fiber surface generated by the different flow rates between PLA melt and ramie fibers. Subsequently, PLA chains in the vicinity of the well-oriented fiber fold into lamellar crystallites perpendicular to the fiber, and finally, the transcrystallinity structure is formed as shown in Figure 1b. In summary, the formation of transcrystallinity originates from the synergetic effect of the shear-aligned fibers and the orientation and stretching of polymer chains.[22,42] A singel fiber-pulling experiment as a model experiment was also conducted to verify this understanding. Showing morphological presentation from POM and SEM observations, Figure 6 compares the transcrystallinity superstructure formed at the ramie fiber under the quiescent and shear flow-induced crystallization, respectively. During the quiescent crystallization, heterogeneous nuclei are sparsely generated at the fiber surface, and fan-shaped transcrystallinity is cylindrically developed around the fiber as shown in Figure 6a and c. By clear contrast, Figure 6b and d reveals that after shearing the PLA melt by gently pulling the pre-embedded ramie fiber numerous nuclei densely locate at the fiber surface. These compact nuclei must be created by the process of shear-induced self-nucleating, taking into consideration the moderate nucleation ability of ramie fiber. Providing the rich self-nucleated nuclei, the subsequent growth of lamellae is largely constrained by the adjacent nuclei, and finally a brush-shaped transcrystallinity texture is developed. This experiment definitely confirmed the synergistic effect of shear flow and ramie fiber on the formation of shear-induced transcrystallinity.

It is worth stressing that nano-sized ramie fibers can induce the hybrid shish-kebab superstructure for PLA, while the shear flow field displays vital significance as the driving force. Currently, the polymer candidates with preferential zigzag chains are typically selected to decorate carbon nanotubes, such as polyethylene and Nylon 6,6.[24] In general, the temperature and endurance time must be strictly controlled to eventually obtain hybrid shish-kebabs for polyethylene, even though polyethylene is a kind of flexible polymer with high steric regularity and favorable crystallization kinetics. By contrast, it is still a great challenge to form hybrid shish-kebabs in biodegradable PLA, which lies in, to a great extent, its short chain length, poor steric regularity, and semi-rigid macromolecular backbone. These intrinsic drawbacks actually drag the PLA crystallization into a dilemma, not to mention the formation of unique hybrid shish-kebab superstructures. Finding the appropriate nanofibers to induce hybrid shish-kebabs for PLA is another key issue. On the basis of ingenious laboratory scale efforts, "size-dependent soft epitaxy" is proposed to describe the main growth for hybrid shish-kebabs of semi-crystalline polymers induced by carbon nanotubes under quiescent states.[19,20,36,43] According to this assumption, a strict lattice matching between the polymer chains and the graphitic sheet is essential for the epitaxy growth of semi-crystalline polymers on larger diameter fibers such as carbon fiber, while geometric confinement might render polymer chains to align along the tube axis regardless of the lattice matching as long as the fiber diameter decreases into the size of the radius of gyration (R_g) of polymers, which is typically approximately 10 nm.[44] In our case, note that due to the poor crystallization kinetics and low steric regularity compared to polyethylene it is practically impossible for a PLA melt to induce the epitaxy growth during rapid cooling of injection molding, regardless of the strict lattice matching and geometric confinement. Thus the "size-dependent soft epitaxy" mechanism cannot perfectly meet with the unique issues herein. Now, how can we explain the unexpected formation of the nano-sized ramie fiber-induced hybrid shish-kebabs driven by the intensive shear flow?

On the basis of morphological observations and quantitative results, we attempt to propose our understanding on this interesting topic. PLA molecular chains tend to deform and stretch under the intense shear flow field, and afterward, these chains highly orient and may pack to form a sequence of quasi-crystalline nanodomains, constituting the inner structure of row-nuclei and shish. The initial row-nuclei in the vicinity of ultrafine ramie fibers are prone to be captured onto the surface, which mainly results from the large surface energy due to the nanostructure.[26] The absorption and stabilization of the oriented row-nuclei can be further enhanced by the physical interactions between the carbonyl groups of PLA and voluminous hydroxyl groups on the nanofiber surfaces.[45] As crystallization proceeds, we can anticipate that nano-sized ramie fibers wrapped with extended chain bundles act as shish units, onto which lamellae may afterward develop to kebabs perpendicular to the hybrid shishes, and finally, hybrid shish-kebabs are formed. We describe this progress as a process of

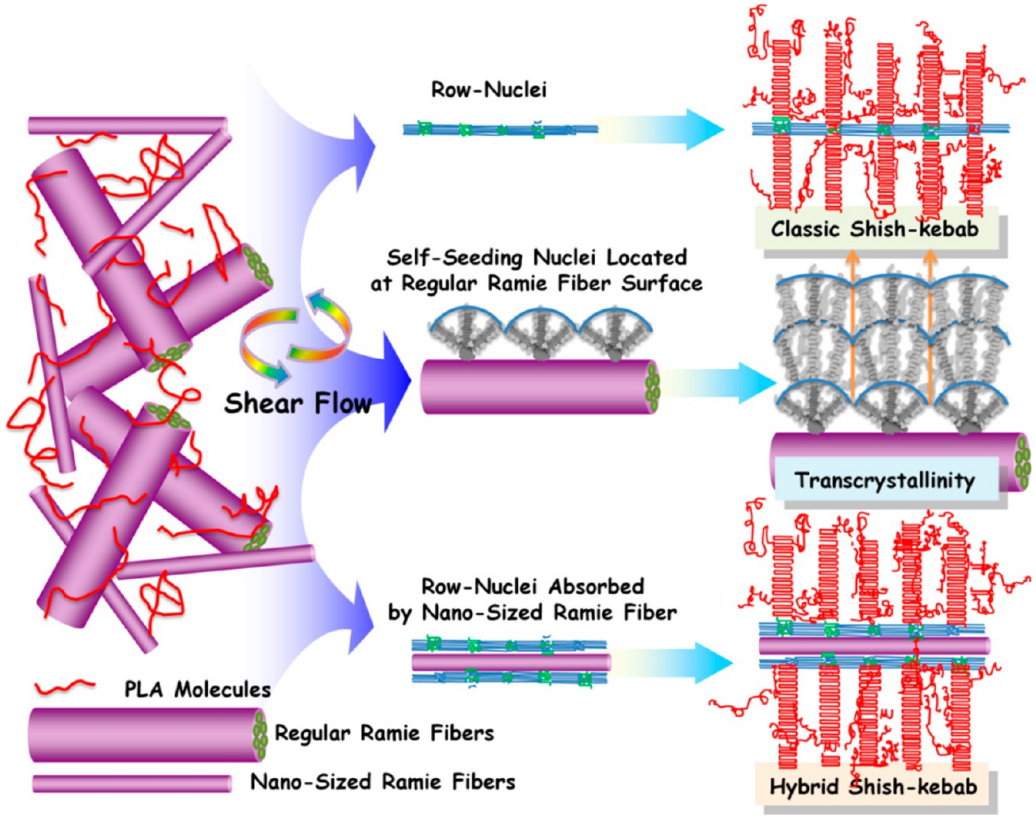

Figure 7. Schematic representation for formation mechanisms of nano-sized ramie fiber-induced hybrid shish-kebab, classic shish-kebab, and ramie fiber-induced transcrystallinity, respectively, while the shear flow acts as the driving force.

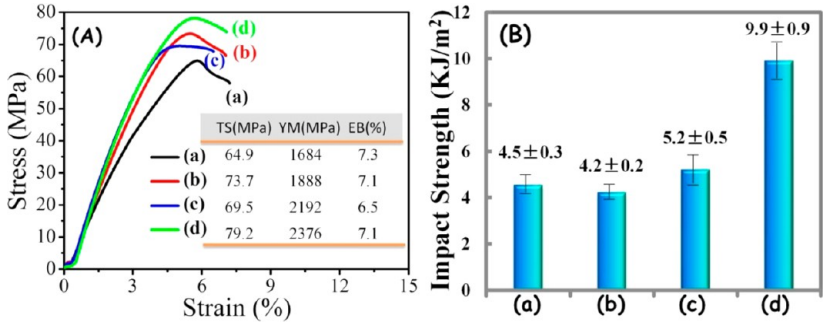

Figure 8. Mechanical properties of (a) C-PLA, (b) O-PLA, (c) C-PLA10, and (d) O-PLA10. (A) Typical stress−strain curves. The inset table summarizes the tensile properties, including tensile strength (TS), Young's modulus (YM), and elongation to break (EB). (B) Impact strength.

"capturing extended chain bundles for hybrid shishes" driven by the applied shear flow. The direct evidence for this proposition is that the diameters of both classic shish-kebabs and hybrid shish-kebabs are in the coincidence of 2 μm, which firmly manifests that classic shish-kebabs and hybrid shish-kebabs must form at the same time and endure a simultaneous growth procedure. A schematic was drawn in Figure 7 to summarize the mechanism for the interesting multiform crystalline superstructures. That is, intense shear flow could induce a certain amount of row nuclei of PLA, especially in the vicinity of a ramie fiber due to amplified effect of shear flow. When they are near the surface of the ramie fiber, they are either absorbed by regular fiber to form a transcrystallinty or captured by nano-sized fiber to form hybrid shish-kebab. If they are far away from the surface of the ramie fiber, classic shish-kebabs tend to form.

Mechanical Performance of Injection-Molded PLA Biocomposites. We find interesting to reveal the performance of PLA biocomposites containing transcrystallinity, shish-kebabs, and hybrid shish-kebabs. Figure 8A shows the typical stress−strain curves of injection-molded PLA and PLA/ramie biocomposites. Obviously, all samples perform in a similar tensile behavior, showing a fracture with slight plastic deformation after the yield point. Some important parameters of the stress−strain curves are summarized in the inset table of Figure 8A. The tensile strength and Young's modulus climb to 73.7 and 1888 MPa for the O-PLA sample and from 64.9 and 1684 MPa for the C-PLA sample. The enhancement derives from the presence of rich shish-kebabs in the O-PLA sample.[16] As for the biocomposite samples, the addition of 10 wt % ramie fibers moderately increases the tensile strength and Young's modulus for C-PLA10 compared to the C-PLA counterpart, achieving 69.5 and 2192 MPa. Furthermore, the most desirable performance exists in the OSIM biocomposite sample; the tensile strength and Young's modulus reach up to 79.2 and

dx.doi.org/10.1021/sc4003032 | ACS Sustainable Chem. Eng. 2013, 1, 1619−1629

2367 MPa, respectively.[15] As for ductility, the PLA samples experience brittle fracture with low elongations at a break of approximately 7%. Although the elongation at break slightly declines to 6.5% for C-PLA10, the ductility of the O-PLA10 sample returns to the same level of the PLA samples with an elongation at break of 7.1%. The desirable ductility mainly lies in the improved efficiency of transferring interfacial stress thanks to the generation of transcrystallinity (Figure S4, Supporting Information). Figure 8B compares the impact strength for the four samples. The C-PLA and O-PLA samples show poor performance in notched impact resistance with the impact strength of approximately 4.5 KJ/m^2, which is moderately promoted to 5.2 KJ/m^2 for the O-PLA10 sample. With some surprise, O-PLA10 performs excellently in impact resistance, achieving a superb level of 9.9 KJ/m^2, which multiplies 2 times compared to those of the PLA samples, which is mainly ascribed to the formation of transcrystallinity and hybrid shish-kebab superstructures and thus improved interfacial adhesion.

The tensile properties and dynamical mechanical performances (Figure S5, Supporting Information) demonstrate the PLA biocomposites with high strength, stiffness, and toughness are successfully prepared under the significant efforts of the intense shear flow. It is imperative and instructive to acquire a further understanding of the reinforcing and toughening mechanism. In general, natural fibers are naturally hydrophilic, while matrix polymers are basically hydrophobic, which likely results in undesirable debonding between the matrix and natural fiber, and eventually causes poor mechanical properties.[46] It has become the main issue in effectively developing natural fiber-reinforced composites. Previous efforts to improve the interfacial properties are mainly concerned with chemical modification of the surfaces of natural fibers, and various alkali solutions and coupling agents have been applied to achieve surface treatment.[30] Unfortunately, this approach must be extremely time consuming and dramatically increase production costs. What is worse is that it essentially goes against our original intention to develop green biocomposites toward dealing with environmental issues and sustainable development.[47−54] Herein, the continuous strong shear flow significantly tailors the crystalline morphology and boosts the crystallinity for PLA. It not only facilitates the preferential formation of shish-kebabs and hybrid shish-kebabs but also creates compact transcrystallinity with oriented lamellae. On the one hand, the existence of compact transcrystallinity and highly oriented shish-kebabs, hybrid shish-kebabs, and ramie fibers will effectively provide high resistance to external loading, and the enhanced interfacial properties allows more effective transfer of applied stress, permitting superb promotion of strength and stiffness for the composite material. On the other hand, the numerous well-aligned ramie fibers, transcrystallinity, and hybrid shish-kebabs are prone to absorb much energy and restrain crack propagation during a sudden impact loading, i.e., growing cracks can be arrested and catastrophic failure is postponed in the aligned fibers and lamellae, thus the impact strength is significantly enhanced. The strengthened interfacial properties in the presence of transcrystallinity is responsible for the improved impact resistance as well.

CONCLUSIONS

In this work, exploiting the strong shear flow during practical processing, multiform crystalline superstructures of PLA were unearthed in the OSIM PLA/ramie fiber biocomposite sample. We successfully enabled the direct formation of a transcrystallinity texture on the fiber surface, shish-kebabs, and hybrid shish-kebabs in the matrix simultaneously at industrial scale. The shish-kebabs presented a dramatically increased diameter compared to those of the OSIM PLA sample, which stemmed primarily from the enhanced shear flow field due to the addition of ramie fibers. Besides the generation of PLA shish-kebabs, the interesting transcrystallinity superstructure was directly formed at the fiber surface, both of which highly benefited the improvement of mechanical properties. More interesting, some ultrafine ramie fibers, coming from the raw ramie directly or generated by mechanical effects during processing, were verified to induce hybrid shish-kebabs for the first time. On the basis of morphological observations and quantitative analyses, we proposed that the process of "capturing extended chain bundles for hybrid shishes" driven by the applied shear flow could be responsible for the formation of hybrid shish-kebabs. Thanks to the synergistic effects of the well-aligned ramie fibers induced by severe shear flow, enhanced fiber/matrix interfacial properties due to the existence of transcrystallinity, and positive reinforcing and toughening effects of shish-kebabs and hybrid shish-kebabs with extended chain bundles, impressive mechanical performance and thermo-mechanical properties were therefore obtained in the OSIM biocomposite sample. It is worth stressing that the exploration herein gives more insights into the crystalline morphology in PLA/natural fiber biocomposites formed during intense shear flow, which might open a promising door to industrially manufacturing absolutely green and superior PLA biocomposites without using any toxic and environmentally harmful reagents.

ASSOCIATED CONTENT

Supporting Information

POM observations of orientation of ramie fibers in injection-molded PLA biocomposites, morphology of nano-sized ramie fiber, and fractured surface for injection-molded PLA/ramie fiber biocomposites observed by SEM, experimental description, and results of dynamic mechanical analysis, and schematic presentation of oscillation shear injection molding. This material is available free of charge via the Internet at http://pubs.acs.org.

AUTHOR INFORMATION

Corresponding Authors

*Phone: +86-28-8540-0211. Fax: +86-28-8540-6866. E-mail: ganji.zhong@scu.edu.cn. (G.-J.Z.).
*Phone: +86-28-8540-6866. Fax: +86-28-8540-6866; E-mail: zmli@scu.edu.cn. (Z.-M.L.).

Notes

The authors declare no competing financial interest.

ACKNOWLEDGMENTS

The authors gratefully appreciate the financial support from the National Natural Science Foundation of China (Grant No. 51120135002, 51121001, 51203104, and 50925311). We also express sincere thanks to the Shanghai Synchrotron Radiation Facility (SSRF, Shanghai, China) for the kind help on 2D-SAXS measurements.

REFERENCES

(1) Dorgan, J. R.; Braun, B.; Wegner, J. R.; Knauss, D. M. Poly(lactic acids): A Brief Review. In *Degradable Polymers and Materials. Principles and Practice*; Khemani, K., Scholz, C., Eds.; ACS Symposium Series 1114; American Chemical Society: Washington, DC, 2006; pp 102−125.

(2) Chung, Y.-L.; Olsson, J. V.; Li, R. J.; Frank, C. W.; Waymouth, R. M.; Billington, S. L.; Sattely, E. S. A renewable lignin−lactide copolymer and application in biobased composites. *ACS Sustainable Chem. Eng.* **2013**, DOI: 10.1021/sc4000835.

(3) Inkinen, S.; Hakkarainen, M.; Albertsson, A.-C.; Södergård, A. From lactic acid to poly(lactic acid) (PLA): characterization and analysis of pla and its precursors. *Biomacromolecules* **2011**, *12*, 523−532.

(4) Nyambo, C.; Mohanty, A. K.; Misra, M. Polylactide-based renewable green composites from agricultural residues and their hybrids. *Biomacromolecules* **2010**, *11*, 1645−1660.

(5) Nagarajan, V.; Mohanty, A. K.; Misra, M. Sustainable green composites: value addition to agricultural residues and perennial grasses. *ACS Sustainable Chem. Eng.* **2013**, *1*, 325−333.

(6) Li, Q.; McGinnis, S.; Sydnor, C.; Wong, A.; Renneckar, S. Nanocellulose life cycle assessment. *ACS Sustainable Chem. Eng.* **2013**, *1*, 919−928.

(7) Satyanarayana, K. G.; Arizaga, G. G. C.; Wypych, F. Biodegradable composites based on lignocellulosic fibers—An overview. *Prog. Polym. Sci.* **2009**, *34*, 982−1021.

(8) Zhang, M.; Xu, J.; Zhang, Z.; Zeng, H.; Xiong, X. Effect of transcrystallinity on tensile behaviour of discontinuous carbon fibre reinforced semicrystalline thermoplastic composites. *Polymer* **1996**, *37*, 5151−5158.

(9) Zhang, S.; Minus, M. L.; Zhu, L.; Wong, C.-P.; Kumar, S. Polymer transcrystallinity induced by carbon nanotubes. *Polymer* **2008**, *49*, 1356−1364.

(10) Klein, N.; Marom, G. Microstructure of nylon 66 transcrystalline layers in carbon and aramid fibre reinforced composites. *Polymer* **1996**, *37*, 5493−5498.

(11) Folkes, M. J.; Hardwick, S. T. Direct study of the structure and properties of transcrystalline layers. *J. Mater. Sci. Lett.* **1987**, *6*, 656−658.

(12) Felix, J. M.; Gatenholm, P. Effect of transcrystalline morphology in interfacial adhesion in cellulose-PP composites. *J. Mater. Sci.* **1994**, *29*, 3043−3049.

(13) Wang, Y.; Tong, B.; Hou, S.; Li, M.; Shen, C. Transcrystallization behavior at the poly(lactic acid)/sisal fibre biocomposite interface. *Compos. Part A: Appl. Sci.* **2011**, *42*, 66−74.

(14) Le Duigou, A.; Davies, P.; Baley, C. Interfacial bonding of flax fibre/poly($_L$-lactide) bio-composites. *Compos. Sci. Technol.* **2010**, *70*, 231−239.

(15) Xu, H.; Liu, C.-Y.; Chen, C.; Hsiao, B. S.; Zhong, G.-J.; Li, Z.-M. Easy alignment and effective nucleation activity of ramie fibers in injection-molded poly(lactic acid) biocomposites. *Biopolymers* **2012**, *97*, 825−839.

(16) Xu, H.; Zhong, G.-J.; Fu, Q.; Lei, J.; Jiang, W.; Hsiao, B. S.; Li, Z.-M. Formation of shish-kebabs in injection-molded poly(l-lactic acid) by application of an intense flow field. *ACS Appl. Mater. Interfaces* **2012**, *4*, 6774−6784.

(17) Tang, H.; Chen, J.-B.; Wang, Y.; Xu, J.-Z.; Hsiao, B. S.; Zhong, G.-J.; Li, Z.-M. Shear flow and carbon nanotubes synergistically induced nonisothermal crystallization of poly(lactic acid) and its application in injection molding. *Biomacromolecules* **2012**, *13*, 3858−3867.

(18) Somani, R. H.; Yang, L.; Zhu, L.; Hsiao, B. S. Flow-induced shish-kebab precursor structures in entangled polymer melts. *Polymer* **2005**, *46*, 8587−8623.

(19) Chen, Y.-H.; Zhong, G.-J.; Wang, Y.; Li, Z.-M.; Li, L. Unusual tuning of mechanical properties of isotactic polypropylene using counteraction of shear flow and β-nucleating agent on β-form nucleation. *Macromolecules* **2009**, *42*, 4343−4348.

(20) Kmetty, Á.; Bárány, T.; Karger-Kocsis, J. Self-reinforced polymeric materials: A review. *Prog. Polym. Sci.* **2010**, *35*, 1288−1310.

(21) Zhong, Y.; Fang, H.; Zhang, Y.; Wang, Z.; Yang, J.; Wang, Z. Rheologically determined critical shear rates for shear-induced nucleation rate enhancements of poly(lactic acid). *ACS Sustainable Chem. Eng.* **2013**, *1*, 663−672.

(22) Larin, B.; Avila-Orta, C. A.; Somani, R. H.; Hsiao, B. S.; Marom, G. Combined effect of shear and fibrous fillers on orientation-induced crystallization in discontinuous aramid fiber/isotactic polypropylene composites. *Polymer* **2008**, *49*, 295−302.

(23) Li, L.; Li, C. Y.; Ni, C. Polymer crystallization-driven, periodic patterning on carbon nanotubes. *J. Am. Chem. Soc.* **2006**, *128*, 1692−1699.

(24) Li, L.; Li, B.; Hood, M. A.; Li, C. Y. Carbon nanotube induced polymer crystallization: The formation of nanohybrid shish−kebabs. *Polymer* **2009**, *50*, 953−965.

(25) Zhang, S.; Lin, W.; Wong, C.-P.; Bucknall, D. G.; Kumar, S. Nanocomposites of carbon nanotube fibers prepared by polymer crystallization. *ACS Appl. Mater. Interfaces* **2010**, *2*, 1642−1647.

(26) Minus, M. L.; Chae, H. G.; Kumar, S. Polyethylene crystallization nucleated by carbon nanotubes under shear. *ACS Appl. Mater. Interfaces* **2012**, *4*, 326−330.

(27) Ljungberg, N.; Wesslén, B. Tributyl citrate oligomers as plasticizers for poly (lactic acid): thermo-mechanical film properties and aging. *Polymer* **2003**, *44*, 7679−7688.

(28) Fischer, E. W.; Sterzel, H. J. Investigation of the structure of solution grown crystals of lactide copolymers by means of chemical reactions. *Kolloid Z. Z. Polym.* **1973**, *251*, 980−990.

(29) Li, H.; Zhang, X.; Kuang, X.; Wang, J.; Wang, D.; Li, L.; Yan, S. A scanning electron microscopy study on the morphologies of isotactic polypropylene induced by its own fibers. *Macromolecules* **2004**, *37*, 2847−2853.

(30) Colom, X.; Carrasco, F.; Pagès, P.; Cañavate, J. Effects of different treatments on the interface of HDPE-lignocellulosic fiber composites. *Compos. Sci. Technol.* **2003**, *63*, 161−169.

(31) Kalay, G.; Sousa, R. A.; Reis, R. L.; Cunha, M.; Bevis, M. J. The enhancement of the mechanical properties of a high-density polyethylene. *J. Appl. Polym. Sci.* **1999**, *73*, 2473−2483.

(32) Kalay, G.; Kalay, C. R. Interlocking shish-kebab morphology in polybutene-1. *J. Polym. Sci., Polym. Phys.* **2002**, *40*, 1828−1834.

(33) Liang, S.; Wang, K.; Yang, H.; Zhang, Q.; Du, R.; Fu, Q. Crystal morphology and tensile properties of LLDPE containing PP fibers as obtained via dynamic packing injection molding. *Polymer* **2006**, *47*, 7115−7122.

(34) Zhang, L.; Tao, T.; Li, C. Formation of polymer/carbon nanotubes nano-hybrid shish−kebab via non-isothermal crystallization. *Polymer* **2009**, *50*, 3835−3840.

(35) Zhang, Z.; Xu, Q.; Chen, Z.; Yue, J. Nanohybrid shish-kebabs: supercritical CO_2-induced PE epitaxy on carbon nanotubes. *Macromolecules* **2008**, *41*, 2868−2873.

(36) Yang, J.; Wang, C.; Wang, K.; Zhang, Q.; Chen, F.; Du, R.; Fu, Q. Direct formation of nanohybrid shish-kebab in the injection molded bar of polyethylene/multiwalled carbon nanotubes composite. *Macromolecules* **2009**, *42*, 7016−7023.

(37) Ma, H.; Burger, C.; Hsiao, B. S.; Chu, B. Ultrafine polysaccharide nanofibrous membranes for water purification. *Biomacromolecules* **2011**, *12*, 970−976.

(38) Kumar, S.; Hofmann, M.; Steinmann, B.; Foster, E. J.; Weder, C. Reinforcement of stereolithographic resins for rapid prototyping with cellulose nanocrystals. *ACS Appl. Mater. Interfaces* **2012**, *4*, 5399−5407.

(39) Jalal Uddin, A.; Araki, J.; Gotoh, Y. Toward "strong" green nanocomposites: polyvinyl alcohol reinforced with extremely oriented cellulose whiskers. *Biomacromolecules* **2011**, *12*, 617−624.

(40) Yang, L.; Somani, R. H.; Sics, I.; Hsiao, B. S.; Kolb, R.; Fruitwala, H.; Ong, C. Shear-induced crystallization precursor studies in model polyethylene. *Macromolecules* **2004**, *37*, 4845−4859.

(41) Balzano, L.; Kukalyekar, N.; Rastogi, S.; Peters, G. W.; Chadwick, J. Crystallization and dissolution of flow-induced precursors. *Phys. Rev. Lett.* **2008**, *100*, 048302.
(42) Wang, K.; Guo, M.; Zhao, D.; Zhang, Q.; Du, R.; Fu, Q.; Dong, X.; Han, C. C. Facilitating transcrystallization of polypropylene/glass fiber composites by imposed shear during injection molding. *Polymer* **2006**, *47*, 8374−8379.
(43) Li, L.; Yang, Y.; Yang, G.; Chen, X.; Hsiao, B. S.; Chu, B.; Spanier, J. E.; Li, C. Y. Patterning polyethylene oligomers on carbon nanotubes using physical vapor deposition. *Nano Lett.* **2006**, *6*, 1007−1002.
(44) Flory, P. J. *Principles of Polymer Chemistry*. Cornell University Press: Ithaca, NY, 1953.
(45) Tingaut, P.; Zimmermann, T.; Lopez-Suevos, F. Synthesis and characterization of bionanocomposites with tunable properties from poly(lactic acid) and acetylated microfibrillated cellulose. *Biomacromolecules* **2010**, *11*, 454−464.
(46) Magniez, K.; Voda, A. S.; Kafi, A. A.; Fichini, A.; Guo, Q.; Fox, B. L. Overcoming interfacial affinity issues in natural fiber reinforced polylactide biocomposites by surface adsorption of amphiphilic block copolymers. *ACS Appl. Mater. Interfaces* **2012**, *5*, 276−283.
(47) Ayoub, A.; Venditti, R. A.; Pawlak, J. J.; Salam, A.; Hubbe, M. A. Novel hemicellulose−chitosan biosorbent for water desalination and heavy metal removal. *ACS Sustainable Chem. Eng.* **2013**, *1*, 1102−1109.
(48) Guo, B.; Chen, W.; Yan, L. Preparation of flexible, highly transparent, cross-linked cellulose thin film with high mechanical strength and low coefficient of thermal expansion. *ACS Sustainable Chem. Eng.* **2013**, DOI: 10.1021/sc400252e.
(49) Dias, A. M. A.; Cortez, A. R.; Barsan, M. M.; Santos, J. B.; Brett, C. M. A.; de Sousa, H. C. Development of greener multi-responsive chitosan biomaterials doped with biocompatible ammonium ionic liquids. *ACS Sustainable Chem. Eng.* **2013**, DOI: 10.1021/sc4002577.
(50) Ghosh Dastidar, T.; Netravali, A. N. Crosslinked waxy maize starch based 'green' composites. *ACS Sustainable Chem. Eng.* **2013**, DOI: 10.1021/sc400113a.
(51) Salam, A.; Lucia, L. A.; Jameel, H. A novel cellulose nanocrystals-based approach to improve the mechanical properties of recycled paper. *ACS Sustainable Chem. Eng.* **2013**, DOI: 10.1021/sc400226m.
(52) Chang, C.-W.; Wang, M.-J. Preparation of microfibrillated cellulose composites for sustained release of h2o2 or o2 for biomedical applications. *ACS Sustainable Chem. Eng.* **2013**, *1*, 1129−1134.
(53) Reddy, N.; Zhang, Y.; Yang, Y. Corn distillers dried grains as sustainable and environmentally friendly warp sizing agents. *ACS Sustainable Chem. Eng.* **2013**, DOI: 10.1021/sc4002017.
(54) Sen, S.; Martin, J. D.; Argyropoulos, D. S. Review of cellulose non-derivatizing solvent interactions with emphasis on activity in inorganic molten salt hydrates. *ACS Sustainable Chem. Eng.* **2013**, *1*, 858−870.